Long-Sought Redox Isomerization of Europium(III/II) Complex Achieved by Molecular Reorientation at the Interface

Alexander V. Shokurov,[†,] Daria S. Kutsybala,[†] Alexander G. Martynov,[†] Artem V. Bakirov,[‡] Maxim A. Shcherbina,[‡] Sergei N. Chvalun,[‡] Yulia G. Gorbunova,[†,§] Aslan Yu. Tsivadze,[†,§] Anna V. Zaytseva,[†] Dmitri Novikov,[‖] Vladimir V. Arslanov,[†] and Sofiya L. Selektor[†]*

† A.N. Frumkin Institute of Physical Chemistry and Electrochemistry of Russian Academy of Sciences, Leninsky pr. 31-4, Moscow, 119071 Russia

‡ Enikolopov Institute of Synthetic Polymeric Materials of Russian Academy of Sciences, Profsoyuznaya 70, Moscow, 117393 Russia

§ N.S. Kurnakov Institute of General and Inorganic Chemistry of Russian Academy of Sciences, Leninsky pr. 31, Moscow, 119071 Russia

‖ Deutsches Elektronen-Synchrotron, PETRA III, Notkestraße 85, Hamburg, D-22607 Germany.

ABSTRACT Redox-isomerism, i.e. the change of metal cation valence state in organic complexes, can find promising applications in multistable molecular switches for various

molecular electronic devices. However, despite a large amount of studies devoted to such processes in organic complexes of multivalent lanthanides, redox-isomeric transformations were never observed for europium. In the present work, we demonstrate the unique case of redox isomerization of Eu(III)/Eu(II) complexes on the example of Eu(III) double-decker octa-*n*-butoxyphthalocyaninate (**Eu[(BuO)$_8$Pc]$_2$**) under ambient conditions (air, room temperature). It is shown that assumption of the face-on orientation on the aqueous subphase surface, in which two of each phthalocyanine decks in **Eu[(BuO)$_8$Pc]$_2$** are located in different media (air and water), leads to the intramolecular electron transfer that results in formation of divalent Eu(II) cation in the complex. Lateral compression of the thus formed monolayer brings on the reorientation of the bisphthalocyaninate to the edge-on state, in which the ligands can be considered identical, and occurrence of the reverse redox-isomeric transformation into the complex with trivalent Eu cation. Both redox-isomeric states were directly observed by XANES spectroscopy in ultrathin films formed under different conditions.

INTRODUCTION

Design of molecular-based electronic and spintronic materials for high density data storage and advanced sensing applications requires implementation of multistable compounds, properties of which can be controlled by various external stimuli.[1,2] Among them, special attention is paid to coordination compounds that can undergo stimulated and reversible intramolecular electron transfer between metal centers and organic ligands, which is known either as redox isomerism or valence tautomerism.

Redox isomerization is typically achieved by thermal action, application of high hydrostatic pressure or magnetic field, irradiation with light or X-rays, etc. This process is accompanied by alteration of optical and magnetic properties of the complexes, which can be read-out by

physical-chemical measurements in order to form the basis of their practical applications.[3,4] This phenomenon is commonly studied on the examples of complexes formed by *d*-metals that are characterized by several accessible redox states – typically, vanadium, manganese, iron, cobalt, nickel, copper, etc, with non-innocent ligands such as diimines, dioxolenes, phenoxyls, tetrapyrrolic macrocycles, etc. Since the first publication in 1980 reporting on valence tautomerization of cobalt complex with semiquinone and dioxolene ligands,[5,6] numerous examples of redox-isomeric *d*-metal complexes were described and comprehensively reviewed.[7–11]

In contrast, the examples of redox-isomerism among electron-rich *f*-element complexes remain exceptional, although almost every lanthanide can form coordination compounds with either trivalent or di-/tetravalent state of the metal center.[12] Binuclear ytterbium complexes with non-innocent bisiminoacenaphthene (bian) ligands were among the first reported examples of lanthanide complexes, where the intramolecular electron transfer between Ln^{3+} and ligand was observed (Figure 1).[13,14] These complexes undergo redox-isomerization $(bian^{2-})Yb^{3+}X \leftrightarrow (bian^{-\bullet})^{-}Yb^{2+}X$ upon temperature change both in solution and in crystalline phase. This transformation became possible particularly due to low potential of Yb^{3+} reduction that leads to a filled $4f^{14}$ shell.[15] Although europium is also characterized by low reduction potential $E°(Eu^{3+}/Eu^{2+})$ providing a stable half-filled $4f^7$ shell, its bian complexes did not exhibit redox isomerization upon similar action,[16,17] and to the best of our knowledge, Eu-based redox-isomeric systems remained unknown.

It should be noted, that among redox-active lanthanides, cerium attracts special attention, since its tetravalent state with closed shell configuration ($4f^0$) is sometimes even more stable than its trivalent counterpart. In coordination compounds, the stability of certain form of Ce cation can

be finely tuned by appropriate ligand surrounding. For example, in the case of double-decker complexes with porphyrin and phthalocyanine ligands, Ce metal center is typically tetravalent, but attains trivalent state in the electron-rich naphthalocyanine surrounding due to the delocalization of electron from the ligands to the metal center, which was quantified by L_{III}-edge X-ray absorption near-edge structure (XANES) profiles.[18] One more example of redox-isomeric transformation of *f*-element compounds was recently discovered by us: crown-substituted cerium bisphthalocyaninate $Ce[(15C5)_4Pc]_2$ revealed unprecedented redox-isomeric behavior, where intramolecular metal-ligand electron transfer was triggered in Langmuir monolayers by change of molecular orientation at the air/water interface.[19] I.e. spreading of its chloroform solution onto the air/water interface and lateral compression of the resulting Langmuir monolayer leads to a reversible redox-isomerization and concomitant interchange between Ce(III)/Ce(IV) states in the monolayer.

In the present work, we exploit this orientation-induced redox-isomerization approach to tune the valent state of the europium cation in double-decker europium(III) octa-n-butoxyphthalocyaninate **$Eu[(BuO)_8Pc]_2$**, in order to achieve Eu(III)/Eu(II) redox isomerization. Apart from fundamental interest in this novel manifestation of redox-isomeric behavior, the described system can pave way to the development of novel optoelectronic devices where the studied bisphthalocyaninates can be incorporated as a functional component in the form of thin solid films.[20–22]

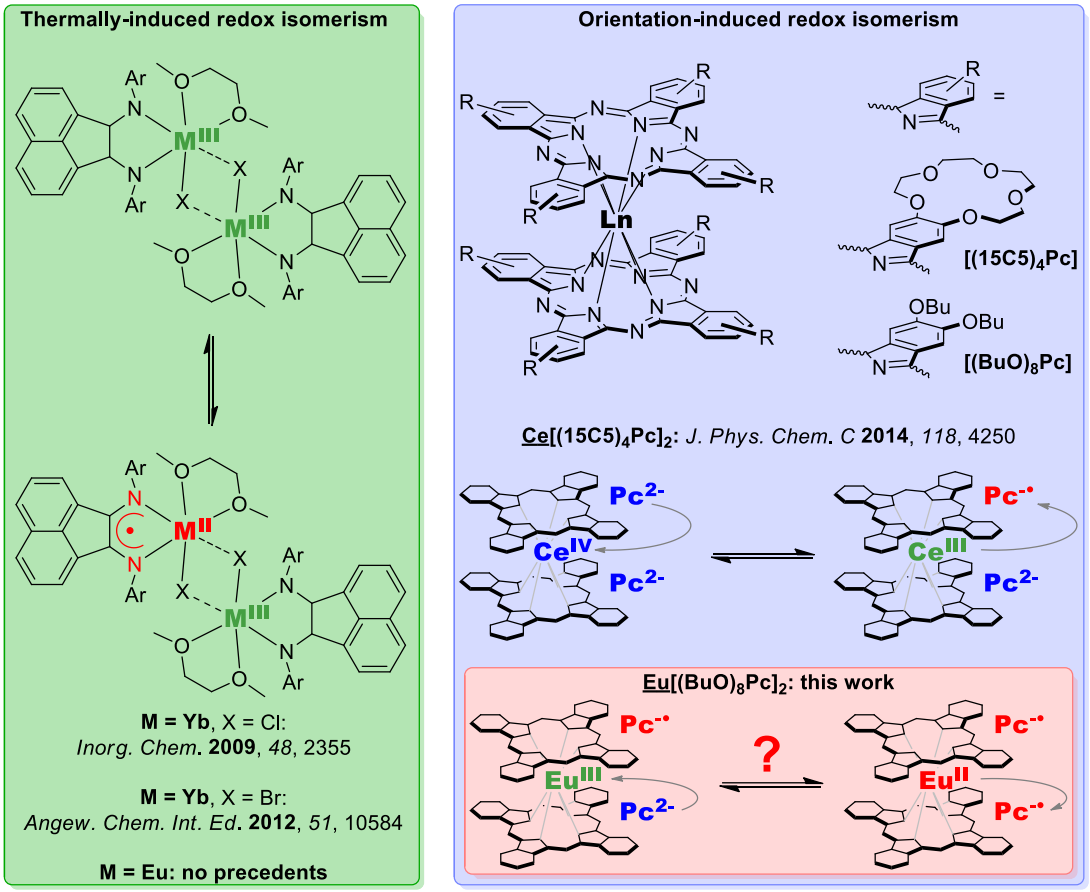

Figure 1. Several examples of lanthanide complexes redox-isomerism and a schematic of electronic changes occurring in lanthanide bisphthalocyaninates upon intramolecular electron transfer.

RESULTS AND DISCUSSION

Analogously to the study of cerium bisphthalocyaninate, on the first stage of the present research we formed Langmuir monolayers of the **Eu[(BuO)8Pc]2** (structure and approximated spatial dimensions are shown in Figure 2) on the surface of deionized water. During this process, we recorded absorbance spectra in the visible range, which are represented in Figure 3 that also shows the absorbance spectrum of the chloroform solution (curve 1) used for the procedure. It can be seen that in the first moments of the spreading, the obtained monolayer spectrum

(curve 2) strongly resembles the one in solution. However, after some time, in which the solvent evaporates from the water surface, the monolayer spectrum begins to change. The prominent change manifests in the redistribution of the Q-band components of the complex between the positions at 681 nm and 721 nm. The kinetics of this process can be conveniently estimated by plotting the dependence of the ratio between the absorbance intensities at designated wavelengths on exposure time. Thus, we can use coefficient K_Q, defined as

$$K_Q = \frac{A_{721}}{A_{681}}, \quad (1)$$

where A_{721} and A_{681} are observed absorbance intensities at 721 and 681 nm, respectively.

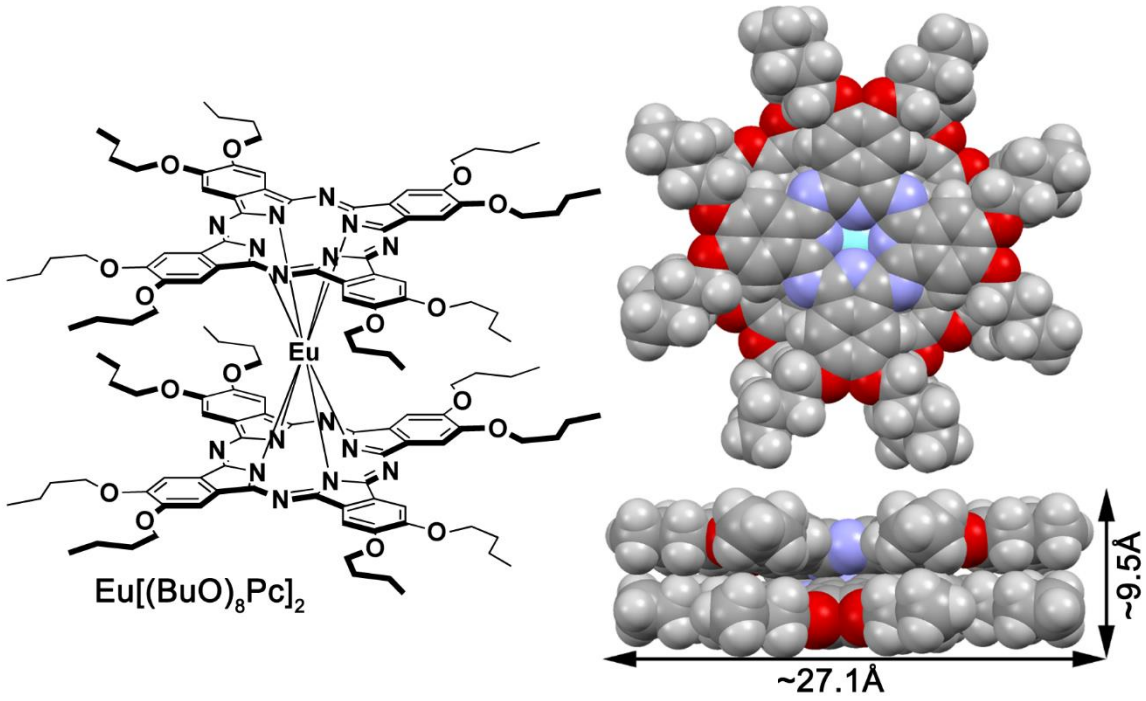

Figure 2. Chemical structure and estimated spatial dimensions of **Eu[(BuO)$_8$Pc]$_2$** complex (calculated by PM6-DH2 method, SPARKLE was used for Eu ion).

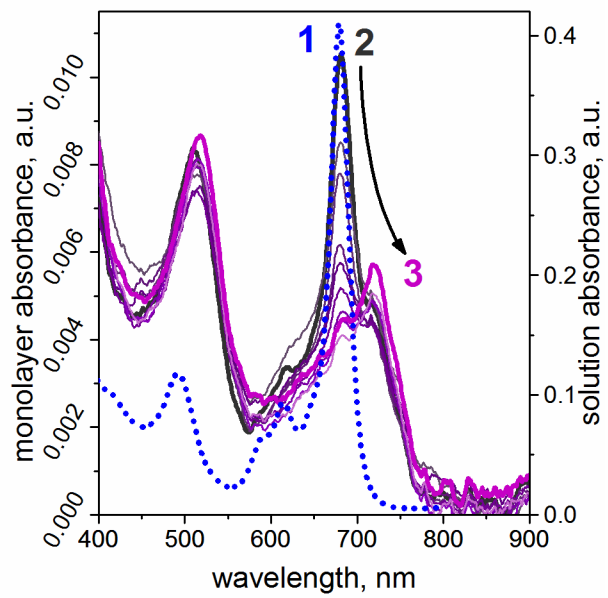

Figure 3. Visible range absorbance spectra of **Eu[(BuO)$_8$Pc]$_2$** in (1) chloroform solution, (2) and (3) monolayer at air/water interface: (2) just after spreading of the solution, and (3) after 10 min of solvent evaporation.

The plot of this coefficient as a function of **Eu[(BuO)$_8$Pc]$_2$** monolayer exposure time is shown in Fig. 4. As can be seen, in the first moments of monolayer formation, the band at 681 nm, also observed in the solution used for monolayer formation, is predominant. However, after *ca.* 4 min, the intensities of the bands under consideration become equal, and after *ca.* 7 min, the ratio K_Q stabilizes at the value around 1.15, which signifies that at this point the band *ca.* 721 nm becomes predominant. No further changes are observed in an undisturbed **Eu[(BuO)$_8$Pc]$_2$** monolayer.

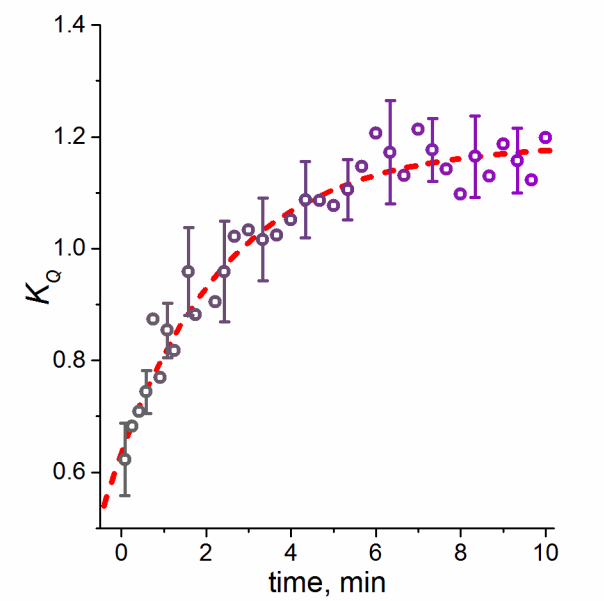

Figure 4. Change of the K_Q value during the solvent evaporation phase of the **Eu[(BuO)$_8$Pc]$_2$** monolayer formation.

As was the case in the study of cerium phthalocyaninate,[19] it can be hypothesized that such change of the spectrum is due to intramolecular electron transfer from the phthalocyanine ligand to the metal center cation, which results in the Eu(II) state (as represented schematically on the right side of Figure 1). Evidently, like in the case of the cerium compound, this is the result of uncompensated surface forces: discotic sandwich complex molecules assume face-on orientation at the interface, when they are given enough space, and in such a way, one of the ligand decks becomes solvated by water from the subphase, while the other one is not. Such conditions make phthalocyanine decks non-equivalent, which in its turn becomes a driving force for the redox-isomeric transformation.

In this light, a possible re-orientation of the phthalocyaninate molecules into edge-on orientation, where both macrocyclic ligands would be equivalent could lead to the reverse intramolecular electron transfer with a low activation barrier. To achieve this, similarly to the

study of redox-isomeric behavior of cerium complexes, one could exploit the natural tendency of tetrapyrrolic compounds to form stacking aggregates in monolayers upon lateral compression.

Figure 5 shows evolution of the absorbance spectra of the **Eu[(BuO)$_8$Pc]$_2$** monolayer upon compression. It is clear that at some point, the band at *ca.* 721 nm ceases to be a dominant feature of the spectrum, and the Q-band at 681 nm reappears. More detailed examination of this process can be performed by analyzing the compression isotherms along with kinetics of spectral changes, i.e. dependence of the ratio K_Q on mean molecular area during compression.

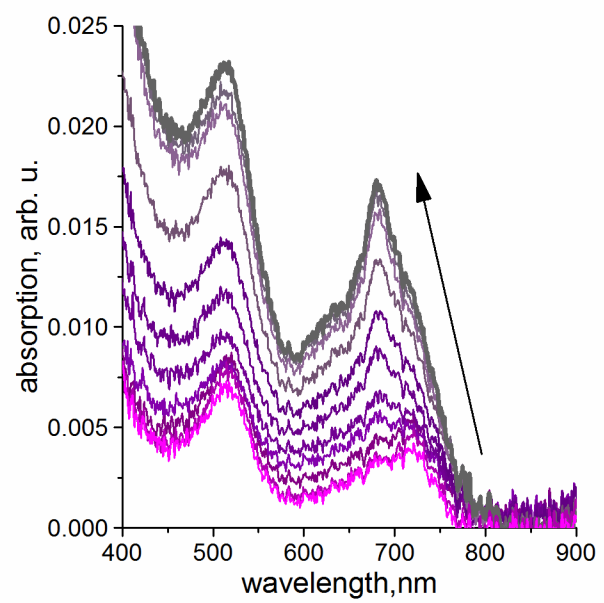

Figure 5. The evolution of the absorbance spectra of **Eu[(BuO)$_8$Pc]$_2$** monolayer upon lateral compression up to surface pressure of 25 mN/m.

A typical $\pi - A$ compression isotherm of the **Eu[(BuO)$_8$Pc]$_2$** monolayer is shown in Figure 6 (curve 1). The first main feature – the onset of surface pressure increase – is observed at *ca.* 560 Å^2, which corresponds to the area of discotic approximation of the **Eu[(BuO)$_8$Pc]$_2$** molecule in a face-on orientation (Figure 2). The bend observed at around 230 Å^2 can be explained by the achievement of the limiting area occupied by a phthalocyanine discotic

molecule in an edge-on orientation. More in depth analysis of these data can be carried out using the dependence of the monolayer compressibility modulus ε on mean molecular area during the compression of the monolayer. The former can be obtained by using the derivative of the $\pi - A$ isotherm, according to a known formula (2).

$$\varepsilon = -A\left(\frac{\partial \pi}{\partial A}\right), \tag{2}$$

where π is surface pressure and A is mean molecular area.

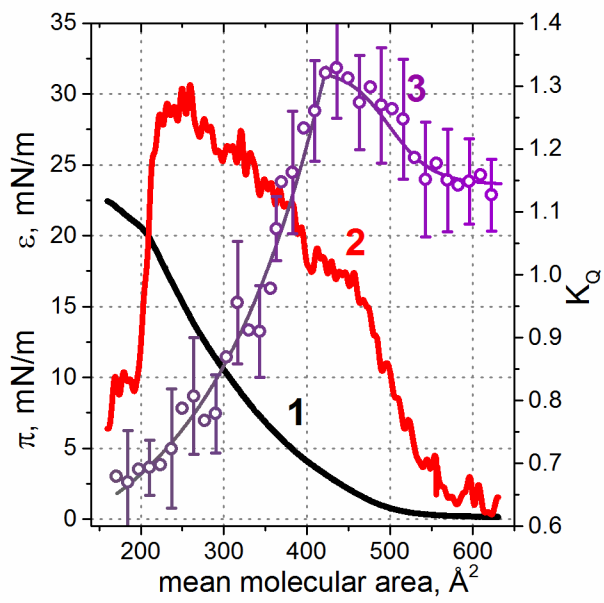

Figure 6. Typical (1) **Eu[(BuO)$_8$Pc]$_2$** monolayer compression isotherm, (2) calculated compressibility modulus, and (3) ratio K_Q at corresponding mean molecular area value.

The obtained dependence is shown in Figure 6, curve 2. As expected both significant mean molecular area values discussed above are well pronounced on this graph in form of sharp increase of compression modulus, when molecules in the monolayer are forced into contact with each other in face-on orientation (*ca.* 560 Å^2), and an abrupt drop, when all phthalocyaninate discs in the monolayer assume edge-on orientation (*ca.* 230 Å^2). However, another feature of this

curve is a significant bend at *ca.* 450 Å^2 that signifies a change of the compressibility of the monolayer after this mean molecular area is reached. Such value is quite hard to associate with any geometrical parameters of the discotic approximation of the **Eu[(BuO)$_8$Pc]$_2$** molecule. It probably corresponds to the limiting area of the molecule that has butoxyl chains interlocked with the neighboring molecules in the monolayer and/or slight decrease of spatial molecular dimensions due to the "flexibility" of the butoxy substituents. In any case, compression after this mean molecular area value should lead to a forced re-orientation of the molecules in the monolayer into edge-on orientation.

What is more interesting is that $K_Q - A$ curve calculated from the spectral data obtained during the compression of **Eu[(BuO)$_8$Pc]$_2$** monolayer (Figure 6, curve 3) plotted in the same graph has a maximum that coincides with the discussed bend on the $\varepsilon - A$ curve. The increase of the K_Q value before this inflection point probably corresponds to the increasing density of the monolayer that in its turn leads to a general increase of the absorbance at 721 nm due to a higher packing of the phthalocyaninate molecules characterized by this band per unit of surface area. However, the steep decrease of the K_Q after *ca.* 450 Å^2 and until the end of compression (where this ratio reaches values close to the ones observed at the first moments of monolayer formation) can be explicitly interpreted as redistribution of the Q-band components in favor of the short wavelength position around 681 nm.

This behavior, like the reverse redox-isomeric transformation of cerium cation described previously,[19] can be explained by the reverse intramolecular electron transfer from the divalent europium center to the phthalocyanine ligand with the formation of Eu(III) state. The coincidence of the mean molecular areas, at which inflections of both $\varepsilon - A$ and $K_Q - A$ curves is observed (*ca.* 450 Å^2), leads to a logical assumption that at this point in monolayer compression,

the densest packing of **Eu[(BuO)$_8$Pc]$_2$** molecules in face-on orientation is achieved. Further compression of the monolayer leads to re-orientation of the bisphthalocyaninate discs into edge-on position, in which both ligands in the sandwich complex are solvated in the same way, and can be considered identical/equivalent. Upon compression, more and more molecules assume this orientation and undergo intramolecular electron transfer back from the metal center to the phthalocyanine ligands that results in the appearance of the complex with a trivalent europium. These orientation changes can be visualized by atomic force microscopy images for the films transferred from monolayers with corresponding organization (data and discussion are provided in Supplementary Information).

To confirm the orientation-induced redox isomerism hypothesis, we formed a **Eu[(BuO)$_8$Pc]$_2$** monolayer on a limited water surface area, in such a way that the mean molecular area in the forming monolayer would not exceed 250 Å^2, thus inhibiting the initial face-on orientation of the molecules. As was expected, the Q-band *ca.* 681 nm position in the spectrum of such monolayer is predominant, and does not change significantly after solvent evaporation during prolonged exposure time. It is interesting to note that cyclic compression–expansion of thus formed monolayer demonstrates reversibility of the above described spectral changes.

On the next stage of the present research we investigated the possibility to form thin films of **Eu[(BuO)$_8$Pc]$_2$** in different redox-isomeric forms on solid substrates. For this, we transferred the studied monolayers onto quartz substrates using Langmuir-Blodgett technique. To obtain samples of **Eu[(BuO)$_8$Pc]$_2$** Langmuir-Blodgett films (LBFs) with exclusively divalent and trivalent metal centers, we transferred the films from Langmuir monolayers formed on large or limited available water surface area, respectively, as was described above. Observed UV-Vis absorbance spectra of these samples confirm that redox-isomeric state mainly persists through

the transfer procedure, as evidenced by the dominant Q-bands in positions respective to the complexes with divalent and trivalent europium metal center (Figure 7). It should be noted that a film formed by drop casting the **Eu[(BuO)$_8$Pc]$_2$** chloroform solution onto a solid substrate (cast film) (Figure 7, curve 3) exhibits a spectrum quite similar to the solution, and by extension to the film formed on a limited available surface area (Figure 7, curve 2), since in both cases europium metal center is trivalent.

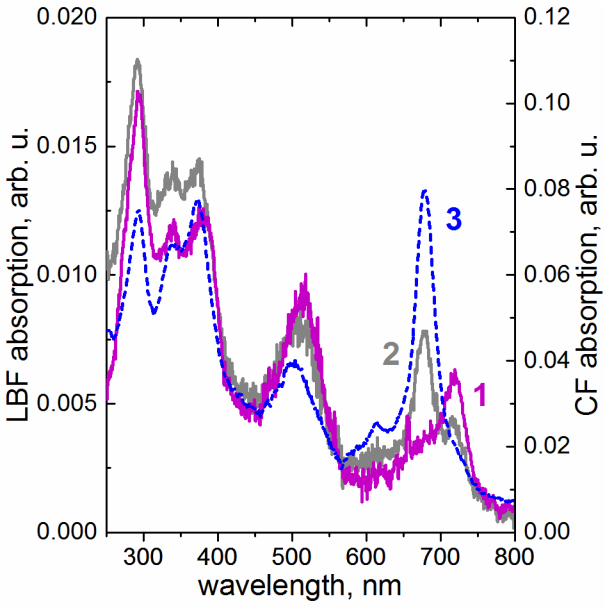

Figure 7. UV-Vis spectra of **Eu[(BuO)$_8$Pc]$_2$** LBFs on quartz substrates, transferred from monolayers formed (1) on large and (2) limited available water surface area, as well as (3) a cast film (CF) formed by drop casting the chloroform solution onto the substrate.

Although spectral data point to the redox-isomeric transformations occurring in the process of monolayer formation and compression, they cannot be regarded as a direct proof of europium metal center valence change. Thus, we employed bright synchrotron source X-ray absorption near edge structure (XANES) technique to determine the valence of the **Eu[(BuO)$_8$Pc]$_2$** metal center in the LBFs, transferred under different conditions onto silicon substrates, as explained above.

Figure 8 shows XANES spectra obtained along europium L_{III}-edge for the studied LBFs on silicon surface, as well as the spectra of the divalent and trivalent inorganic Eu references used (Figure 8, a and b, respectively). As can be seen from the graph, the spectrum of the thick film formed by drop-casting the **Eu[(BuO)$_8$Pc]$_2$** chloroform solution onto silicon substrate (Figure 8, curve 1) clearly corresponds to the absorption of trivalent Eu, which is the state the metal center exists in solution and without any effect of the air/water interface. The LBF obtained from the monolayer formed on the limited water surface area, in which case the visible absorbance spectra corresponded to the complex with trivalent metal center, exhibits analogous absorption edge profile, thus confirming again the trivalent state of europium cation in this case as well. However, the XANES spectrum of an LBF transferred from a true Langmuir monolayer formed with large available mean molecular area clearly resembles the form of the X-ray absorption edge of the divalent reference. These data directly confirm the existence of divalent europium phthalocyaninate complexes under ambient conditions in the studied ultrathin films. Moreover, it shows that the change of the discotic **Eu[(BuO)$_8$Pc]$_2$** molecules orientation at the air/water interface causes the intramolecular electron transfer from the ligand to the metal center and back.

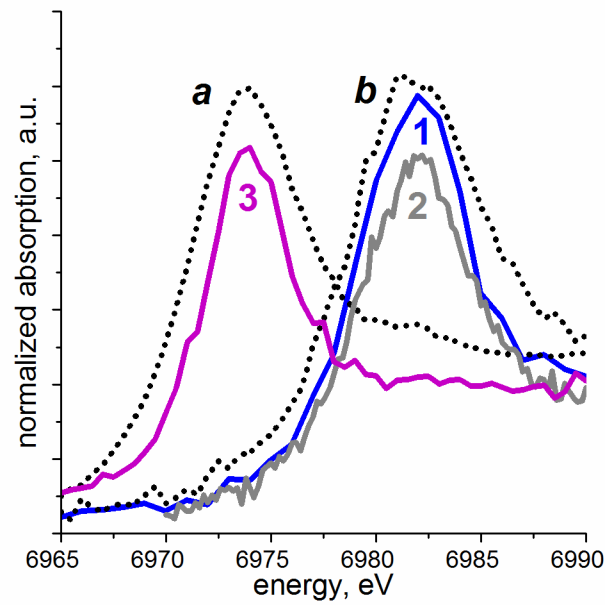

Figure 8. XANES spectra for **Eu[(BuO)$_8$Pc]$_2$** (1) cast film, and LBFs obtained from Langmuir monolayers formed on (2) limited and (3) large available surface area upon formation. Dotted curves correspond to the XANES spectra of inorganic references used: (a) $EuSO_4$ and (b) Eu_2O_3.

Interestingly, during XANES measurements, it was observed that the divalent metal cations of the respective **Eu[(BuO)$_8$Pc]$_2$** films undergo transformation into trivalent ones under exposure to the synchrotron X-ray radiation. This way, the oxidation state of the Eu cation changes almost completely from Eu^{2+} to Eu^{3+} in the matter of 20 minutes upon exposition to the monochromatic radiation with the energy of 7 keV, as illustrated by the evolution of their XANES spectra in Figure 9. This is probably due to the metastable nature of the phthalocyaninate complex with divalent metal center. It should be noted, however, that in absence of X-ray radiation, the samples with Eu^{2+} are stable for at least a week under ambient conditions as evidenced by UV-Vis spectra. At this moment, it is unclear, if such metastable state can be stabilized in low temperature and/or inert atmosphere environment, since all the presented studies were performed in air at room temperature. Chemical modification of the phthalocyanine ligand core by more electron donor or acceptor substituents can be an attractive way to shift this equilibrium towards

stable divalent or trivalent redox-isomers. Further research would be devoted to the studies of planar supramolecular systems based on phthalocyanine complexes with different substituents and lanthanide metal centers.

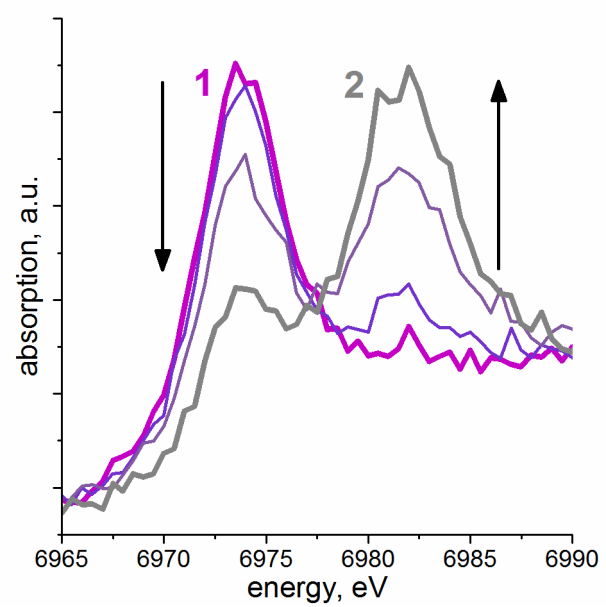

Figure 9. Evolution of XANES spectra of (1) **Eu[(BuO)$_8$Pc]$_2$** LBF with divalent metal center in initial state and (2) after 20 minutes of exposition to X-ray radiation.

CONCLUSIONS

Thus, in the present study we show that transition from the bulk solution of **Eu[(BuO)$_8$Pc]$_2$**, where the europium cation is trivalent, to the air/water interface leads to the intramolecular electron transfer from the phthalocyanine ligands to the metal cation, resulting in the complex with divalent metal center. This is due to the fact that, given enough area, the molecules of the studied compound are oriented in the face-on manner at the interface, thus making the phthalocyanine macrocycles not equivalent, since one of them is solvated by water from the subphase, while the other one is surrounded by air. Such orientation provides the right conditions for the formation of the complex with divalent Eu due to intramolecular electron transfer from

the phthalocyanine ligand to the metal center cation. Lateral compression of the **Eu[(BuO)$_8$Pc]$_2$** monolayer at the air/water interface leads to re-orientation of the discotic molecules into edge-on position, where both ligands can be considered equivalent. In this case, a reverse transformation from Eu^{2+} to Eu^{3+} metal center is observed due to intramolecular electron transfer from the metal cation to the phthalocyanine ligand.

Both Langmuir monolayers of **Eu[(BuO)$_8$Pc]** complexes containing divalent or trivalent Eu cations were successfully transferred onto solid substrates with retention of the respective oxidation states, which were directly confirmed by means of X-ray absorption near edge structure spectroscopy. Thus, we demonstrate for the first time, a redox-isomeric transformation of an organic europium complex that results in a divalent europium cation, where the controlled change of the lanthanide oxidation states occurs under ambient conditions.

EXPERIMENTAL

The studied compound was synthesized according to the previously described procedure.[23]

Geometry optimization was performed using MOPAC2016[24] with PM6-DH2 method containing dispersion correction,[25,26] and SPARKLE for Eu^{3+} ion.[27]

For Langmuir-Blodgett experiments and formation of drop cast films, the studied **Eu[(BuO)$_8$Pc]$_2$** phthalocyaninate was solubilized at a concentration in the range of 1-1.5 10^{-5} M in $CHCl_3$ (HPLC grade, ethanol-stabilized, acquired from Sigma-Aldrich).

Langmuir–Blodgett device KSV Minitrough (Finland) with PTFE trough with surface area of 273.0 cm^2 and moveable barriers made of hydrophilic polyacetal was used for Langmuir monolayer formation. Compression isotherms were recorded using automated Langmuir balance and platinum Wilhelmi plate. The monolayers were formed by spreading the studied solutions onto the air/water interface using a chromatographic syringe. Then the system was left

undisturbed for 10-15 min in order for the solvent to evaporate from the interface. After that, monolayer compression at the rate of 5 mm min^{-1} commenced. Transfer of Langmuir monolayers onto solid substrates was carried out by Langmuir-Blodgett technique (vertical transfer) using an automated dipper device at surface pressures of around 5 mN/m and 15 mN/m in case of monolayers containing divalent and trivalent europium complexes, respectively, as described in Results and Discussion section. All studied LB films were single-layered. Ultrapure water (18 MΩ cm) deionized by Millipore Milli-Q water purification system was used as a subphase in Langmuir monolayer studies.

Absorbance spectra of **Eu[(BuO)$_8$Pc]$_2$** monolayers on aqueous subphase were recorded in the wavelength range of 370−800 nm using an AvaSpec-2048 optic fiber spectrophotometer equipped with halogen light source AvaLight HAL (Avantes, The Netherlands). According to the previously described technique,[28] a reflectometric probe with a fiber diameter of 400 μm combined with a six-fiber irradiating cable was placed perpendicularly to the subphase surface at a distance of 2−3 mm from the monolayer. The signal obtained upon light reflection from the aqueous subphase surface immediately before the monolayer spreading was used as baseline.

Absorption spectra of **Eu[(BuO)$_8$Pc]$_2$** solutions, Langmuir-Blodgett, and drop cast films on quartz substrates were measured in the wavelength range of 220−900 nm using a Shimadzu 2450 PC spectrophotometer (Japan).

X-ray absorption near edge structure (XANES) measurements were carried out at the in situ and nano X-ray diffraction beamline P23 at the PETRA III storage ring at the Deutsches Elektronen-Synchrotron DESY. The X-ray beam from a spectroscopic undulator was monochromatized by a cryogenically cooled double crystal Si(111)/Si(111) monochromator. Two B4C covered flat mirrors were used for harmonics rejection. Due to the very low

concentration of the target atoms in the samples, the XANES data were recorded in the fluorescence detection mode with an Amptek XR100SDD silicon drift detector.

Atomic force microscopy studies were conducted on a Multimode V (Veeco, USA) and HA_NC brand (TipsNano, Zelenograd, Russia) silicon AFM tips (standard geometry, needle height 10 μm, point radius < 10 nm, resonance frequency 235 kHz). All measurements were done in tapping mode, air and room temeprature. Several images throughout the sample area were performed. Processing of the AFM data and height profile acquirement were done using Gwyddion 2.45 software package.

All experiments were carried out under ambient conditions: air atmosphere, air and subphase temperature of 20±1°C.

ASSOCIATED CONTENT

Supporting Information

Supporting Information file contains atomic force microscopy images for the studied LBFs and brief discussion of the data obtained.

AUTHOR INFORMATION

Corresponding Author

*shokurov@phyche.ac.ru.

Funding Sources

The present work was supported Russian Foundation for Basic Research grant No. 18-33-20187 mol_a_ved (Langmuir-Blodgett, spectroscopic and AFM studies) and Russian Science Foundation project No.19-73-20236 (synchrotron research).

ORCID

Alexander V. Shokurov 0000-0003-4562-8603

Daria S. Kutsybala 0000-0002-7732-8368

Alexander G. Martynov 0000-0002-2192-7134

Artem V. Bakirov 0000-0003-0798-2791

Maxim A. Shcherbina 0000-0002-5569-958X

Sergei N. Chvalun 0000-0001-9405-4509

Yulia G. Gorbunova 0000-0002-2333-4033

Aslan Yu. Tsivadze 0000-0001-5601-440X

Vladimir V. Arslanov 0000-0003-4885-1616

Sofiya L. Selektor 0000-0002-3720-1717

Notes

The authors declare no competing financial interest.

ACKNOWLEDGMENT

We acknowledge DESY (Hamburg, Germany), a member of the Helmholtz Association HGF, for the provision of experimental facilities. Analytical measurements were partially performed using equipment of CKP FMI IPCE RAS.

REFERENCES

(1) Martynov, A. G.; Safonova, E. A.; Tsivadze, A. Y.; Gorbunova, Y. G. Functional Molecular Switches Involving Tetrapyrrolic Macrocycles. *Coord. Chem. Rev.* **2019**, *387*, 325–347.

(2) Vittal, J. J.; Quah, H. S. Engineering Solid State Structural Transformations of Metal Complexes. *Coord. Chem. Rev.* **2017**, *342*, 1–18.

(3) Boskovic, C. Valence Tautomeric Transitions in Cobalt-Dioxolene Complexes. In *Spin-Crossover Materials*; Halcrow, M. A., Ed.; John Wiley & Sons Ltd: Oxford, UK, 2013; pp 203–224.

(4) Vázquez-Mera, N. A.; Novio, F.; Roscini, C.; Bellacanzone, C.; Guardingo, M.; Hernando, J.; Ruiz-Molina, D. Switchable Colloids, Thin-Films and Interphases Based on Metal Complexes with Non-Innocent Ligands: The Case of Valence Tautomerism and Their Applications. *J. Mater. Chem. C* **2016**, *4* (25), 5879–5889.

(5) Buchanan, R. M.; Pierpont, C. G. Tautomeric Catecholate-Semiquinone Interconversion via Metal-Ligand Electron Transfer. Structural, Spectral, and Magnetic Properties of (3,5-Di-Tert-Butylcatecholato)(3,5-Di-Tert-Butylsemiquinone)(Bipyridyl)Cobalt(III), a Complex Containing Mixed-Valence. *J. Am. Chem. Soc.* **1980**, *102* (15), 4951–4957.

(6) Li, B.; Zhao, Y.-M.; Kirchon, A.; Pang, J.-D.; Yang, X.-Y.; Zhuang, G.-L.; Zhou, H.-C. Unconventional Method for Fabricating Valence Tautomeric Materials: Integrating Redox Center within a Metal–Organic Framework. *J. Am. Chem. Soc.* **2019**, *141* (17), 6822–6826.

(7) Hendrickson, D. N.; Pierpont, C. G. Valence Tautomeric Transition Metal Complexes. In *Spin Crossover in Transition Metal Compounds II*; Springer-Verlag, 2004; Vol. 1, pp 63–95.

(8) Tezgerevska, T.; Alley, K. G.; Boskovic, C. Valence Tautomerism in Metal Complexes: Stimulated and Reversible Intramolecular Electron Transfer between Metal Centers and

Organic Ligands. *Coord. Chem. Rev.* **2014**, *268*, 23–40.

(9) Drath, O.; Boskovic, C. Switchable Cobalt Coordination Polymers: Spin Crossover and Valence Tautomerism. *Coord. Chem. Rev.* **2018**, *375*, 256–266.

(10) Abakumov, G. A.; Razuvaev, G. A.; Nevodchikov, V. I.; Cherkasov, V. K. An EPR Investigation of the Thermodynamics and Kinetics of a Reversible Intramolecular Metal-Ligand Electron Transfer in Rhodium Complexes. *J. Organomet. Chem.* **1988**, *341* (1–3), 485–494.

(11) Abakumov, G. A.; Cherkasov, V. K.; Nevodchikov, V. I.; Kuropatov, V. A.; Yee, G. T.; Pierpont, C. G. Magnetic Properties and Redox Isomerism for 4,4'-Bis(Semiquinone) Complexes of Copper. *Inorg. Chem.* **2001**, *40* (10), 2434–2436.

(12) MacDonald, M. R.; Bates, J. E.; Ziller, J. W.; Furche, F.; Evans, W. J. Completing the Series of +2 Ions for the Lanthanide Elements: Synthesis of Molecular Complexes of Pr 2+ , Gd 2+ , Tb 2+ , and Lu 2+. *J. Am. Chem. Soc.* **2013**, *135* (26), 9857–9868.

(13) Fedushkin, I. L.; Maslova, O. V; Morozov, A. G.; Dechert, S.; Demeshko, S.; Meyer, F. Genuine Redox Isomerism in a Rare-Earth-Metal Complex. *Angew. Chem. Int. Ed. Engl.* **2012**, *51* (42), 10584–10587.

(14) Fedushkin, I. L.; Maslova, O. V.; Baranov, E. V.; Shavyrin, A. S. Redox Isomerism in the Lanthanide Complex [(Dpp-Bian)Yb(DME)(Mu-Br)]2 (Dpp-Bian = 1,2-Bis[(2,6-Diisopropylphenyl)Imino]Acenaphthene). *Inorg. Chem.* **2009**, *48* (6), 2355–2357.

(15) Cotton, S. The Lanthanides - Principles and Energetics. In *Lanthanide and Actinide Chemistry*; John Wiley & Sons, Ltd: Chichester, UK, 2006; pp 9–22.

(16) Fedushkin, I. L.; Skatova, A. A.; Yambulatov, D. S.; Cherkasov, A. V.; Demeshko, S. V. Europium Complexes with 1,2-Bis(Arylimino)Acenaphthenes: A Search for Redox Isomers. *Russ. Chem. Bull.* **2015**, *64* (1), 38–43.

(17) Fedushkin, I. L.; Yambulatov, D. S.; Skatova, A. A.; Baranov, E. V.; Demeshko, S.; Bogomyakov, A. S.; Ovcharenko, V. I.; Zueva, E. M. Ytterbium and Europium Complexes of Redox-Active Ligands: Searching for Redox Isomerism. *Inorg. Chem.* **2017**, *56* (16), 9825–9833.

(18) Bian, Y.; Jiang, J.; Tao, Y.; Choi, M. T. M.; Li, R.; Ng, A. C. H.; Zhu, P.; Pan, N.; Sun, X.; Arnold, D. P.; et al. Tuning the Valence of the Cerium Center in (Na)Phthalocyaninato and Porphyrinato Cerium Double-Deckers by Changing the Nature of the Tetrapyrrole

Ligands. *J. Am. Chem. Soc.* **2003**, *125* (40), 12257–12267.

(19) Selektor, S. L.; Shokurov, A. V.; Arslanov, V. V.; Gorbunova, Y. G.; Birin, K. P.; Raitman, O. A.; Morote, F.; Cohen-Bouhacina, T.; Grauby-Heywang, C.; Tsivadze, A. Y. Orientation-Induced Redox Isomerism in Planar Supramolecular Systems. *J. Phys. Chem. C* **2014**, *118* (8), 4250–4258.

(20) Shokurov, A. V.; Kutsybala, D. S.; Martynov, A. G.; Raitman, O. A.; Arslanov, V. V.; Gorbunova, Y. G.; Tsivadze, A. Y.; Selektor, S. L. Modulation of Transversal Conductivity of Europium(III) Bisphthalocyaninate Ultrathin Films by Peripheral Substitution. *Thin Solid Films* **2019**, *692*, 137591.

(21) Chen, Y.; Kong, X.; Lu, G.; Qi, D.; Wu, Y.; Li, X.; Bouvet, M.; Sun, D.; Jiang, J. The Lower Rather than Higher Density Charge Carrier Determines the NH3-Sensing Nature and Sensitivity of Ambipolar Organic Semiconductors. *Mater. Chem. Front.* **2018**, *2* (5), 1009–1016.

(22) Jiang, J.; Ng, D. K. P. A Decade Journey in the Chemistry of Sandwich-Type Tetrapyrrolato−Rare Earth Complexes. *Acc. Chem. Res.* **2009**, *42* (1), 79–88.

(23) Oluwole, D. O.; Yagodin, A. V.; Mkhize, N. C.; Sekhosana, K. E.; Martynov, A. G.; Gorbunova, Y. G.; Tsivadze, A. Y.; Nyokong, T. First Example of Nonlinear Optical Materials Based on Nanoconjugates of Sandwich Phthalocyanines with Quantum Dots. *Chem. Eur. J.* **2017**, *23* (12), 2820–2830.

(24) Stewart, J. J. P. MOPAC2016 (Molecular Orbital PACkage). Http://Openmopac.Net/MOPAC2016.Html.

(25) Řezáč, J.; Fanfrlík, J.; Salahub, D.; Hobza, P. Semiempirical Quantum Chemical PM6 Method Augmented by Dispersion and H-Bonding Correction Terms Reliably Describes Various Types of Noncovalent Complexes. *J. Chem. Theory Comput.* **2009**, *5* (7), 1749–1760.

(26) Korth, M.; Pitoňák, M.; Řezáč, J.; Hobza, P. A Transferable H-Bonding Correction for Semiempirical Quantum-Chemical Methods. *J. Chem. Theory Comput.* **2010**, *6* (1), 344–352.

(27) Freire, R. O.; Simas, A. M. Sparkle/PM6 Parameters for All Lanthanide Trications from La(III) to Lu(III). *J. Chem. Theory Comput.* **2010**, *6* (7), 2019–2023.

(28) Stuchebryukov, S. D.; Selektor, S. L.; Silantieva, D. A.; Shokurov, A. V. Peculiarities of

the Reflection-Absorption and Transmission Spectra of Ultrathin Films under Normal Incidence of Light. *Prot. Met. Phys. Chem. Surfaces* **2013**, *49* (2), 189–197.

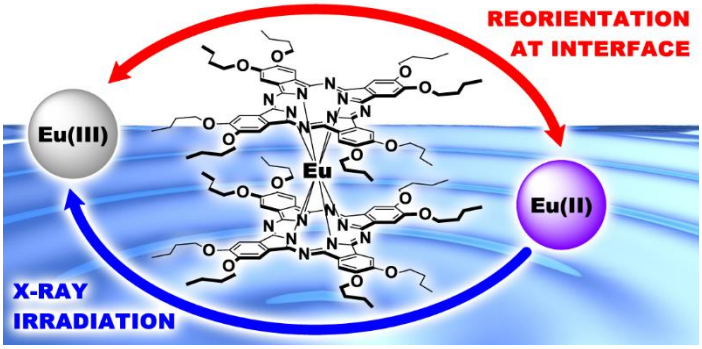

Table of Content graphic